Fission Modes and Mass Distribution in Heavy Actinide Region Studied with Multi-Dimensional Langevin Equation

Takatoshi ICHIKAWA
Advanced Science Research Center, Japan Atomic Energy Research Institute
Tokai-mura, Naka-gun, Ibaraki 319-1195, Japan
e-mail: takichi@popsvr.tokai.jaeri.go.jp

Tomomasa ASANO, Takahiro WADA, Masahisa OHTA
Department of Physics, Konan University
Okamoto 8-9-1, Kobe 658-8501, Japan

We evaluate the mass-energy distribution with the 3-dimensinal Langevin equation in the potential energy surface including the shell correction. From the analysis of our results, we expect the existence of several modes in the fission of ^{270}Sg. We show that the dynamical effect plays an important role with respect to the components of the asymmetric mode with low-TKE.

I. Introduction

In the fission of low excited actinides and transactinides, mass and total kinetic energy (TKE) distributions consisting of some components were observed. These experimental results exhibit the presence of different deformation paths, which is well reviewed in several articles [1,2]. The aim of this study is the reproduction of the mass and TKE distribution and the investigation of the dynamical fission paths obtained by the numerical calculation.

For example, the measurement of the mass-energy distribution of the fission fragments of ^{270}Sg was performed by Itkis *et al.* [3]. It was observed that in the low energy fission, the mass-asymmetric components with low-TKE appear, whereas this component vanishes in the case of the high excitation energy. It appears that in the low energy fission, the shell effect has a very important role.

The problem of fission modes has been studied theoretically as well [4,5]. The multi-dimensional energy surface was calculated with Strutinsky's shell correction method and the search for the saddle points and the valley paths leading to fission in the multi-dimensional energy surface was performed. These static methods reproduce the fission paths expected from the experimental result. However, this is insufficient for the evaluation of the mass and TKE distribution.

Therefore, we propose a dynamical approach by solving the multi-dimensional Langevin equation numerically on the energy surface including the shell correction. In the high excitation energy where the shell effect vanishes, the fission process has been studied on the basis of the fluctuation-dissipation dynamics and the Langevin equation has been succeed in describing this dynamics. By including the shell correction energy to the potential

energy surface, we apply this method to the fission of the low excitation energy.

In this paper, we show the mass distribution of fission fragments of ^{270}Sg at the excitation energy E*=28 MeV by solving the three-dimensional Langevin equation. The origin of the mass-asymmetric component with low-TKE is investigated in terms of the fission paths obtained by numerical calculation. The influence of the potential energy on the dynamics is also discussed.

II. Framework

The shape of nucleus is described by the two-center parameterization. Z_0 denotes the distance between the harmonic oscillators in the unit of the radius of the spherical compound nuclei $\left(R_0 = r_0 \left(A_1 + A_2\right)^{1/3}\right)$, δ denotes the deformation of the fragments with the constraint that both fragments have same deformation ($\delta_1 = \delta_2$) and α the mass asymmetry parameter ($\alpha = \left(A_1 - A_2\right) / \left(A_1 + A_2\right)$), where A_1 and A_2 are the mass number of the fragments. The liquid drop energy, the surface energy and the coulomb energy are also calculated with this parameterization.

We describe the fission process by the following equation, called as the Langevin equation,

$$\begin{aligned} \frac{dq_i}{dt} &= \left(m^{-1}\right)_{ij} p_j, \\ \frac{dp_i}{dt} &= -\frac{\partial V}{\partial q_i} - \frac{1}{2}\frac{\partial}{\partial q_i}\left(m^{-1}\right)_{jk} p_j p_k - \gamma_{ij}\left(m^{-1}\right)_{jk} p_k + g_{ij} R_j(t), \end{aligned} \tag{1}$$

where the suffix stands for Z_0, δ or α. Summation over repeated indices is implied. $V(q)$ is the potential energy taken account of shell effect, $m_{ij}(q)$ and $\gamma_{ij}(q)$ are the shape dependent collective inertia and dissipation tensors, respectively. We assume the random forces as the white noise type of which the normalized random force $R(t)$ is to satisfy $\langle R(t)\rangle$=0, $\langle R_i(t_1) R_j(t_2)\rangle = 2\delta_{ij}\delta(t_1 - t_2)$. The strength of random force g_{ij} is calculated from $\gamma_{ij} T = g_{ik} g_{kj}$ that is given by the fluctuation-dissipative theorem. T denotes the temperature of the compound nucleus that is defined as $E^* = aT^2$ with the excitation energy E^* of a compound nucleus and the level density parameter a of Töke and Swiatecki [6]. The inertia tensor is calculated using the hydrodynamical model with Werner-Wheeler approximation [7] for the velocity field, and wall-and-window one-body dissipation [8] is adopted for the dissipation tensor.

The shell correction energy of the two-center shell model is calculated with the code TWOCTR [9, 10]. The shell correction energy depends on the temperature of the nucleus. The temperature dependent factor of the shell correction energy is assumed as $\exp\left(-E^*/E_d\right)$, where E_d is the shell damping energy that is taken to be 20 MeV [11].

III. Numerical Results and Discussion

We study the fission of the compound nucleus of ^{270}Sg in the case of the excitation energy E*=28 MeV and the origin of the mass-asymmetric fission modes from the analysis of dynamical fission paths obtained by the numerical solution of the 3-dimensional

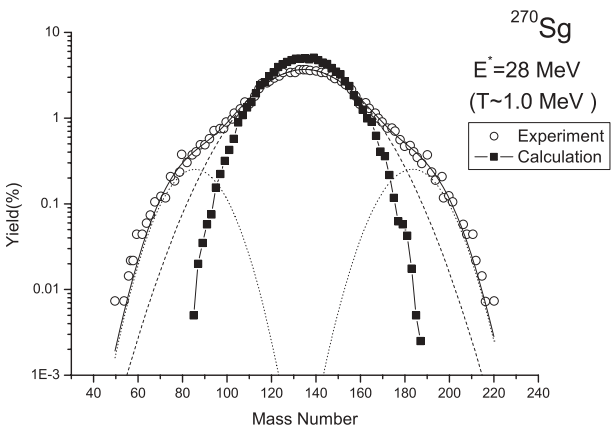

Figure 1: Mass distribution of the fission fragments of ^{270}Sg. The open circle and solid square denote the experimental and the numerical results, respectively.

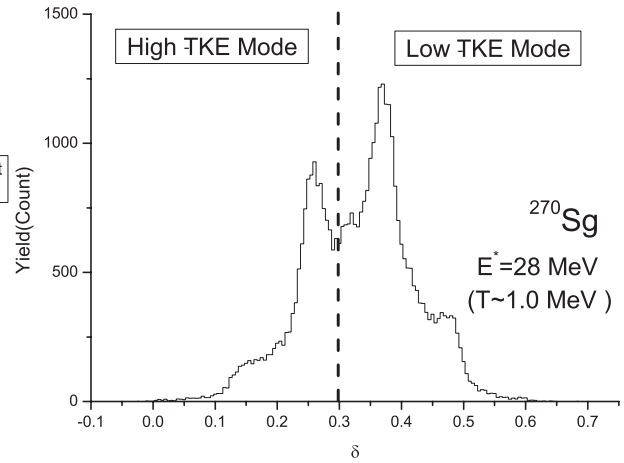

Figure 2: Deformation distribution of the fission fragments at scission configuration.

Langevin equation.

Figure 1 shows the mass distribution of the fission fragments as a function of the mass number of the fission fragments. The open circle and the solid square denote the experimental result and our numerical one, respectively. We obtain the mass distribution with the single peak, whereas it is seen that the experimental mass distribution consists of some Gaussian-components. In our result, the fission fragments with the large mass asymmetry are underestimated. In the experiment [3], the quasi-fission component was not separated in terms of the measurement of the angular distribution of fission fragments. We expect that this underestimation of our results comes from the mixture of the quasi-fission component in the experimental data.

In order to evaluate the quasi-fission component in the experimental data, we perform three-Gaussian fitting for the mass distribution of the experimental result. The mass-symmetric component is denoted by the dashed line and the mass-asymmetric components are denoted by the dotted lines in Figure 1. From the analysis of the TKE distribution, the mass-asymmetric component has the low TKE and differs from the characteristic of the fission mode in the region of the actinide nucleus. It is expected that this asymmetric component comes from the quasi-fission. In this paper, we focus on the distribution coming from the fission of the compound nucleus corresponding to the dashed line in Figure 1 and the investigation is restricted to fission modes with mass number around 80-190.

Figure 2 shows the deformation distribution of the fission fragment at the scission configuration. It seems that the mass distribution of our results consists of the single component, whereas two peaks is clearly seen at δ=0.25 and 0.36 in the deformation distribution. From the calculation in the liquid-drop energy surface without the shell

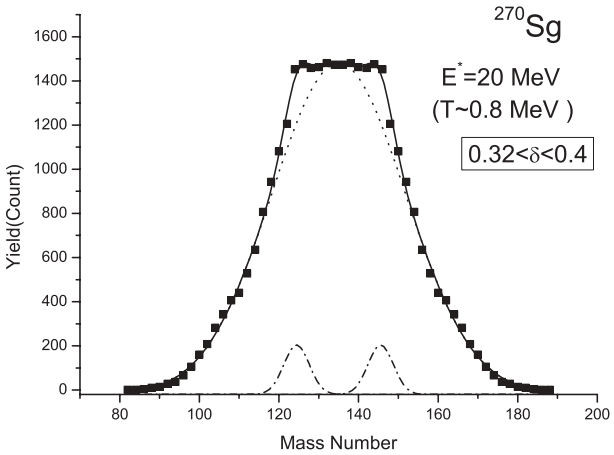

Figure 3: Mass distribution of the fission fragments with the deformation $0.32<\delta<0.4$.

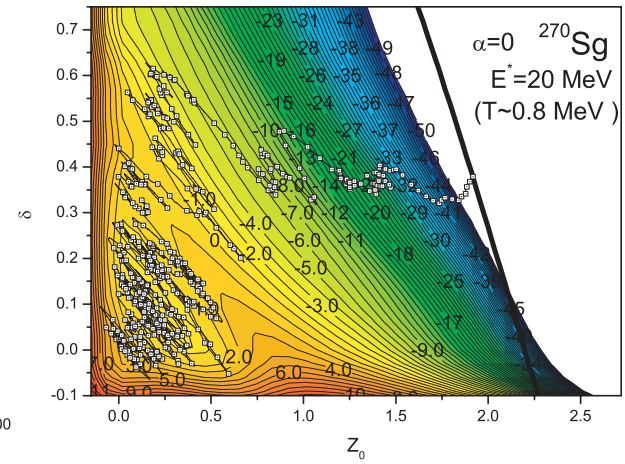

Figure 4: Landscape of the potential energy of ^{270}Sg projected to Z_0-δ plane at α=0.0 with the sample trajectory.

correction, it seems that the peak at δ=0.36 corresponds to the liquid-drop like mode. It is expected that the peak at δ=0.26 appears due to the shell effect. The mass distribution of the events with the deformation $\delta<0.3$ has a very sharp single peak and the average of the TKE value is high compared with the liquid-drop like fission. This is because of the contribution of the components with the peak at δ=0.26 affected by the shell effect.

On the other hand, the mass distribution of the events with $\delta>0.3$ is the liquid drop like one. However, the mass-asymmetric component appears in the liquid-drop like distribution. In order to see the shell effect clearly, we perform the calculation at the excitation energy E*=20 MeV. This corresponds to the increase of the shell correction energy by 50%. Figure 3 shows the mass distribution of the events with $0.32<\delta<0.4$ in the case of E*=20 MeV. We obtain the mass distribution having the flat top. In order to estimate the mixture of the components, we perform three-Gaussian fitting for this mass distribution. The solid line denotes the result of the fitting with three-Gaussian. The dotted line denotes the main Gaussian component used in the fitting. The peak of the dotted line is at 135, *i.e.* this is the mass symmetric division and is the liquid-drop like component. The peaks of the mass-asymmetric components denoted by the dash-dotted lines are at 144 and 125. We expect that this mass-asymmetric component corresponds to the standard II mode proposed by Itkis *et al.* [3]. In the following, we discuss this mass-asymmetric component that appears in the liquid-drop like distribution.

We consider the origin of this mass-asymmetric component. Although the dynamical motion is calculated in the three-dimensional parameter space, it is instructive to look at the potential surface projected onto two-dimensional spaces like Z_0-α and Z_0-δ. We show the time evolution of the deformation of the sample trajectory in this mode. Figure 4 shows the sample trajectory in the mass-asymmetric component with low-TKE and the potential energy landscape projected to the Z_0-δ plane at α=0. The solid line with the

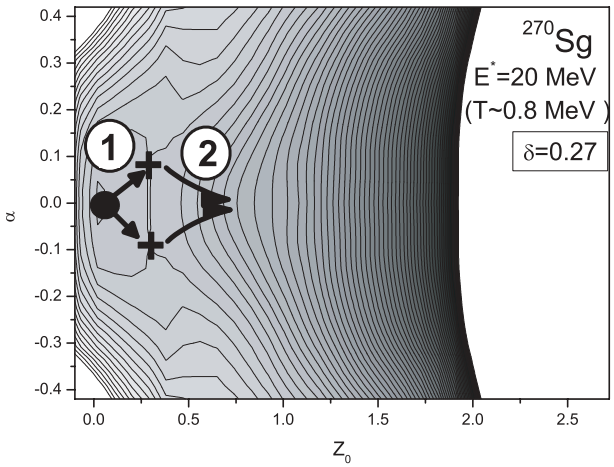

Figure 5: Landscape of the potential energy of ^{270}Sg projected to Z_0-α plane at δ=0.27.

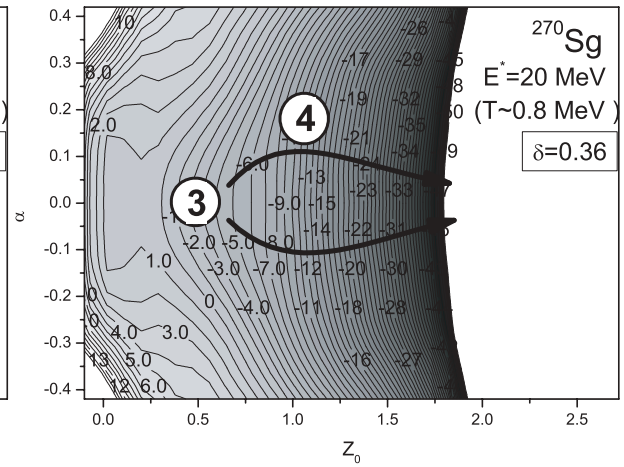

Figure 6: Landscape of the potential energy of ^{270}Sg projected to Z_0-α plane at δ=0.36.

squares denotes the sample trajectory of the mass-asymmetric exit channel at δ=0.36 that corresponds to the one of peaks of the distribution shown in Figure 2.

At first, the Brownian particle remains around the ground state. Receiving the random force from the heat bath, the Brownian particle goes through the first saddle point around at δ=0.27. The deformation δ increases with Z_0 until δ=0.65. After it passes through Z_0=0.5, δ decrease to 0.36. Finally, the Brownian particle goes to the scission line with random-walking.

Figure 5 shows the potential projected to the Z_0-α at δ=0.27 that corresponds to the saddle point deformation in the Z_0-δ plane of Figure 4. Figure 6 shows the potential projected to Z_0-α at δ=0.36 that corresponds to the maximum of the distribution in Figure 4. In the Z_0-α plane, the saddle point is around at Z_0=0.25 and α=$\pm$0.1. First, in Figure 5, when the fissile nucleus goes from the ground state to the saddle point according to the potential surface, the mass asymmetry α increases (the arrow 1). After passing through the saddle point (the cross), the fissile nucleus goes toward scission and Z_0 and δ increase. At the same time, α decreases following the potential slope as shown by the arrow 2 in Figure 5. As is seen from the sample trajectory in Figure 4, after passing through the saddle point, the deformation δ increases from 0.25 to 0.65 with large fluctuation while the increase of Z_0 is relatively small(around the number 3 in Fig. 6). With the increase of δ, the bump due to the shell effect becomes prominent at Z_0 =0.75 and α=0 in Figure 5. Since the Brownian particle keeps away from this bump, the mass asymmetry α increases again (the arrow 4) and the fissile nucleus goes to the asymmetric direction. This is how the asymmetry of fission fragments is determined.

It should be noted that the potential around Z_0=1.2$\sim$2.0 is very flat in α direction in the present system. In addition, the mass asymmetry α at the scission point differs from the one at the saddle point. Therefore, it is inappropriate to determine the mass

asymmetry α by the potential valley; the dynamics after the saddle point plays a very important role for the determination of the mass asymmetry at scission. The mass asymmetry distribution cannot be evaluated only from the position of the saddle point such as the discussion with the static calculation. Thus, we conclude that the dynamical calculation is very important for the understanding of the mass distribution and the fission paths.

Acknowledgements

The authors would like to express his gratitude to Dr. Yuichiro Nagame for his helpful suggestions. The authors wish to thank Prof. Hiromichi Nakahara (Tokyo Metropolitan University) for his valuable advises from the early stage of this study. We wish to thank Dr. Shuhei Yamaji (The Institute of Physical and Chemical Research) for his valuable advises and discussions.

References

[1] *"Fifty Years Research in Nuclear Fission"*, Nucl. Phys. **A502**, (1989).

[2] P. Armbruster, Rep. Prog. Phys. **62**, 465 (1999).

[3] M. G. Itkis *et al.*, Phys. Rev. C **59**, 3172 (1999).

[4] V. V. Pashkevich, Nucl. Phys. **A477**, 1 (1988).

[5] P. Möller, R. Nix, and W. J. Swiatecki, Nucl. Phys. **A469**, 1 (1987).

[6] J. Tōke and W. J. Światecki, Nucl. Phys. **A372**, 141 (1981).

[7] H. J. Krappe, J. R. Nix, and A. J. Sierk, Phys. Rev. C **20**, 992 (1979).

[8] J. R. Nix and A. J. Sierk, Phys. Rev. C **15**, 2072 (1977).

[9] S. Suekane, A. Iwamoto, S. Yamaji, and K. Harada, JAERI-memo. 5948 (1974).

[10] A. Iwamoto, S. Yamaji, S. Suekane, and K. Harada, Prog. Theor. Phys. **55**, 115 (1976).

[11] A. V. Ignatyuk, G. N. Smirenkin, and A. S. Tishin, Sov. J. Nucl. Phys. **21**, 255 (1975).